European Journal of Pharmaceutical Sciences 91 (2016) 64–73

Contents lists available at ScienceDirect

European Journal of Pharmaceutical Sciences

journal homepage: www.elsevier.com/locate/ejps

The development of a peak-time criterion for designing controlled-release devices

Laurent Simon [a,*], Juan Ospina [b]

[a] Otto H. York Department of Chemical, Biological and Pharmaceutical Engineering, New Jersey Institute of Technology, Newark, NJ 0702, USA
[b] Logic and Computation Group, Physics Engineering Program, School of Sciences and Humanities, EAFIT University, Medellin, Colombia

ARTICLE INFO

Article history:
Received 23 April 2016
Received in revised form 20 May 2016
Accepted 29 May 2016
Available online 31 May 2016

Keywords:
Mathematical models
Diffusion
Controlled release
Peak time

ABSTRACT

This work consists of estimating dynamic characteristics for topically-applied drugs when the magnitude of the flux increases to a maximum value, called peak flux, before declining to zero. This situation is typical of controlled-released systems with a finite donor or vehicle volume. Laplace transforms were applied to the governing equations and resulted in an expression for the flux in terms of the physical characteristics of the system. After approximating this function by a second-order model, three parameters of this reduced structure captured the essential features of the original process. Closed-form relationships were then developed for the peak flux and time-to-peak based on the empirical representation. Three case studies that involve mechanisms, such as diffusion, partitioning, dissolution and elimination, were selected to illustrate the procedure. The technique performed successfully as shown by the ability of the second-order flux to match the prediction of the original transport equations. A main advantage of the proposed method is that it does not require a solution of the original partial differential equations. Less accurate results were noted for longer lag times.

1. Introduction

The time it takes for a drug to reach a peak level (t_{max}) in a given compartment, after it is administered, is called the time-of-peak concentration (C_{max}). This parameter is important for assessing the onset of action for a particular medication. The maximum concentration is often termed the peak-height concentration and must be achieved for a patient to respond to a drug (Allen and Ansel, 2014). If one considers the minimum effective concentration (MEC), t_{max} can help clinicians decide which formulation to recommend. For example, if a rapid onset of action is needed, a low t_{max} in the blood plasma is preferred because drugs from this formulation reach the MEC quickly. Bioequivalence is often assessed using C_{max} and t_{max} among other pharmacokinetic parameters. Weidekamm et al. (1998) showed an important difference in the bioequivalence of Mephaquin® (Mepha) compared to Lariam® (Roche), both containing mefloquine hydrochloride. Lariam exhibits about twice the maximum plasma concentration of Mephaquin (C_{max} of 1018 ng/ml vs. 656 ng/ml) and takes nearly one-third of the time to reach C_{max} (t_{max} of 13 vs. 46 h) (Gutman et al., 2009; Weidekamm et al., 1998). These numbers are either read from laboratory data (Urso et al., 2002) or derived from model equations for drugs taken orally (Hedaya, 2012).

Much interest in bioequivalence studies has been directed toward understanding the area under the plasma concentration-time curve (AUC), C_{max} and t_{max}. Other researchers have tried to extract similar useful information from the flux-time profile when dealing with controlled-released devices. In the case of a finite dosage absorbed through the skin layers, the flux approaches zero at infinite time. As a result, it is not possible to determine characteristics, such as the lag time, from a routine graphical method (Crank, 1975). The notion of an effective time concept (Collins, 1980; Simon, 2009) would fail to explain clinical observations satisfactorily in such cases. In fact, a careful analysis of the data would point to the peak flux (j_{max}) and the time-to-peak (t_{jmax}) as the two most relevant dynamic performance parameters. There are important clinical implications for estimating j_{max} and t_{jmax}. These measures are used in in-vitro studies to compare pharmaceutical products. A 10% SEPA® (2-n-nonyl-1,3-dioxolane) formulation containing 5% ibuprofen performed better than several commercial forms based on j_{max}, t_{jmax} and the total drug delivery (Walters, 2002). The same criteria were applied to show that SEPA was also a more effective skin penetration enhancer than Azone for ketoprofen (Walters, 2002). Results from these investigations are indispensable for the development of more accurate in vitro-in vivo correlations.

A number of studies have focused on identifying key properties of a drug that influence j_{max} and t_{jmax}. Early experiments showed a maximum in the flux-time curve when a limited amount of benzoic acid was applied to the surface of the skin: j_{max} increased with the specific dose (Scheuplein and Ross, 1974). The authors noted that for molecules diffusing slowly through the skin (i.e., small diffusion coefficient), efforts to increase j_{max}, by

* Corresponding author.

http://dx.doi.org/10.1016/j.ejps.2016.05.028
0928-0987/

manipulating the dose, may be fruitless. They proposed the following equations:

$$j_{\max} = \frac{1.85DC_0h}{\delta^2} = 1.85\frac{\text{dose}}{At_d} \tag{1}$$

and

$$t_{\max} = \frac{\delta^2 - h^2}{6D} \tag{2}$$

where D is the diffusion coefficient, C_0 is the donor concentration, h is the thickness of the applied drug layer, δ is the stratum corneum thickness, *dose* is the dose size, A is the surface area and t_d is the characteristic time for diffusion (δ^2/D). Edward and Prausnitz (2001) later noticed that as the membrane-to-water distribution coefficient increased, the peak flux of drugs topically delivered to the cornea was expected to rise, reach a maximum and then decrease because of the opposing effects of improved permeability and reduced aqueous solubility.

Other researchers developed mathematical models and proposed solution strategies to help relate $j_{\max}$ and $t_{j\max}$ to physicochemical properties of the device. For the most part, the approaches adopted are akin to what is recommended for compartmental models and can be summarized as follows: i) solve for the flux to get an analytical expression, ii) set the time derivative of the flux equal to zero, iii) solve for the time when the maximum occurs and iv) replace the value of $t_{j\max}$ in the flux expression to get $j_{\max}$. Anissimov and Roberts (2001) carried out this method to analyze percutaneous absorption kinetics for a finite vehicle volume and solvent-deposited solids. However, they were quick to notice that numerical algorithms were needed for parts i) and iii), as stated above, unless certain assumptions were made about the process or a trial-and-error approach was taken. The difficulty lies in the fact that controlled-release phenomena are governed by partial differential equations. As a result, techniques for computing $j_{\max}$ and $t_{j\max}$ can only be developed on a case-by-case basis. In this contribution, we introduce a general scheme to calculate these parameters as a function of key physicochemical properties for finite-release volumes. The main advantage of the procedure is that it does not require a closed-form solution for the flux or a computation of $t_{j\max}$ from the time derivative.

2. Theory

The analysis is first conducted via Laplace transforms. The idea is to approximate the dynamics of a process, which reaches a peak flux, by a function $F(s)$ having the following properties:

$$\lim_{s\to 0}(sF(s)) = \lim_{s\to\infty}(sF(s)) = 0 \tag{3}$$

Eq. (3) guarantees that the initial and final values of the function $f(t)$ (i.e., the inverse Laplace of $F(s)$ are zero. The function $F(s)$ should be made simple to allow efficient analytical estimation of the maximum value of $f(t)$ but complex enough to represent a large class of functions. A candidate function is

$$F(s) = \frac{k}{(s+a)(s+b)} \tag{4}$$

which yields two time constants $1/a$ and $1/b$. It can be shown that

$$f(t) = k\left(\frac{e^{-bt}}{a-b} - \frac{e^{-at}}{a-b}\right) \tag{5}$$

after some manipulations. In addition, we have the following peak time and maximum value, respectively:

$$t_{\max} = \frac{\ln(a/b)}{a-b} \tag{6}$$

and

$$f_{\max} = \frac{\left(\frac{a}{b}\right)^{-\frac{b}{a-b}}k}{a} \tag{7}$$

Another important observation is that the limit of $F(s)$ as s approaches zero is

$$\lim_{s\to 0}\left[\frac{k}{(s+a)(s+b)}\right] = \frac{k}{ab} \tag{8}$$

If $J(s)$ is the model to be approximated by $F(s)$, $f(t)$ represents the inverse Laplace transform of $J(s)$ (i.e.,$j(t)$) fairly well. The following steps are proposed to estimate k, a and b.

- The limit of $F(s)$as s approaches zero is

$$\lim_{s\to 0}[J(s)] = \frac{k}{ab} \tag{9}$$

- The parameters a and b are obtained by creating a power series expansion of $1/J(s)$ around the point $s=0$ to order s^2:

$$\frac{1}{J(s)} \approx \frac{1}{F(s)} = \text{Series}\left(\frac{1}{J(s)}, \{s, 0, 2\}\right) = c_0 + c_1 s + c_2 s^2 \tag{10}$$

By setting Eq. (10) to zero and solving for the roots, we have

$$a = \frac{c_1 + \sqrt{c_1^2 - 4c_0c_2}}{2c_2} \tag{11}$$

and

$$b = \frac{c_1 - \sqrt{c_1^2 - 4c_0c_2}}{2c_2} \tag{12}$$

The constants a, b and k are obtained from Eqs. (9), (11) and (12) and written in terms of the model parameters. The metrics $t_{\max}$ and $f_{\max}$, which can be calculated from Eqs. (6) and (7), fully characterize $j(t)$. An alternative to using Eq. (9) is to apply the limit to Eq. (10):

$$\lim_{s\to 0}\left[\frac{1}{J(s)}\right] = c_0 \tag{13}$$

Note that the analysis of controlled-release devices does not generally lead to two-compartment pharmacokinetic models, which are associated with bi-exponential profiles (Eq. (5)). However, a solution to these release problems is often composed of an infinite series of exponential terms (Crank, 1975). The first Eigen-values are usually sufficient to describe the problem. The technique proposed here goes beyond converting a diffusion-based governing equation to a compartmental model. Such methods are described in the work by McCarley and Bunge (2001). In fact, if the goal was to simply obtain $t_{\max}$ and $f_{\max}$, a graphical or regression method would be less tedious and save time and effort. The issue, addressed in this contribution, is to develop a first-principles-based framework for writing $t_{\max}$ and $f_{\max}$, in terms of critical system parameters, such as diffusion or partition coefficients. Such design relations are based on governing equations that best describe drug release through the device. The application of a graphical or a regression technique to estimate $t_{\max}$ and $f_{\max}$ using laboratory data would fail to link $t_{\max}$ and $f_{\max}$ to the system properties. Three case studies are presented below to illustrate the new concept.

3. Results and discussions

3.1. The percutaneous absorption model of Anissimov and Roberts (2001)

3.1.1. Governing equations for the percutaneous absorption (Model 1)

Transport from a donor to a receiver includes three steps: i) first-order transfer of the molecules from the donor cell to the surface of the stratum corneum (sc) or biological membrane; ii) diffusion to the interface between the sc and the receiver and iii) first-order transport from this boundary into the receiver chamber (Fig. 1). The governing equations are given below (Anissimov and Roberts, 2001).

$$\frac{\partial C_m(x,t)}{\partial t} = D_m \frac{\partial^2 C_m(x,t)}{\partial x^2} \tag{14}$$

$$C_m(x,0) = 0 \tag{15}$$

$$-D_m \frac{\partial C_m(x,t)}{\partial x}\bigg|_{x=0} = k_p^d \left(C_d(t) - \frac{C_m(0,t)}{K_m} \right) \tag{16}$$

$$V_d \frac{dC_d(t)}{dt} = AD_m \frac{\partial C_m(x,t)}{\partial x}\bigg|_{x=0} \tag{17}$$

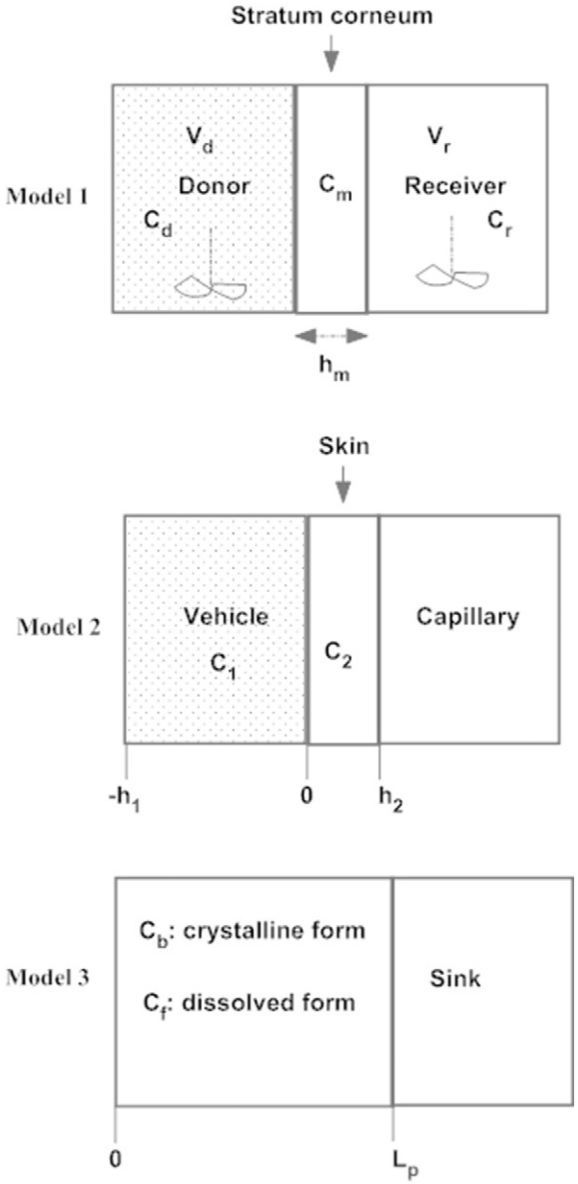

Fig. 1. Graphical representations of the three models. Model 1 shows the percutaneous absorption of a drug. Model 2 describes drug released from a patch. Model 3 involves diffusion and dissolution of the pharmaceutical ingredient.

$$-D_m \left.\frac{\partial C_m(x,t)}{\partial x}\right|_{x=h_m} = k_p^{ve}\left(\frac{C_m(h_m,t)}{K_m} - \frac{C_r(t)}{K_r}\right) \tag{18}$$

$$V_r \frac{dC_r(t)}{dt} = -AD_m \left.\frac{\partial C_m(x,t)}{\partial x}\right|_{x=h_m} - Cl_r C_r(t) \tag{19}$$

$$C_d(0) = C_{d0} \tag{20}$$

$$C_r(0) = 0 \tag{21}$$

$$j(t) = -D_m \left.\frac{\partial C_m(x,t)}{\partial x}\right|_{x=h_m} \tag{22}$$

Eq. (14) describes diffusion through the membrane where C_m is the drug concentration and D_m the diffusion coefficient. Initially, the sc is void of the drug (Eq. (15)). A flux continuity condition is imposed at $x=0$ (i.e., the interface donor/membrane) (Eq. (16)); k_p^d and K_m are the permeability coefficient and the partition coefficient between the two regions, respectively; C_d is the concentration in the donor compartment. The solute is depleted from the latter phase in accordance with Eq. (17). In this equation, V_d is the donor cell volume and A denotes the area occupied by the applied dose. The flux continuity condition is again written at $x=h_m$ (i.e., the interface membrane/receiver) (Eq. (18)); k_p^{ve}, and K_r are the solute permeability at the membrane surface and the equilibrium partition coefficient between the receiver and donor; C_r is the receiver cell concentration. The rate of accumulation of drugs in the receiver is equal to the input rate from the sc and the rate of elimination (Eq. (19)); V_r is the receiver volume and Cl_r a removal rate. No solute molecules are in the donor and receiver at the beginning of the experiments (Eqs. (20) and (21)). Eq. (22) describes the release rate at $x=h_m$.

The dimensionless forms of Eqs. (14)–(21) are given below.

$$\frac{\partial c_m(x_1,\tau)}{\partial \tau} = \frac{\partial^2 c_m(x_1,\tau)}{\partial {x_1}^2} \tag{23}$$

$$c_m(x_1,0) = 0 \tag{24}$$

$$-\left.\frac{\partial c_m(x_1,\tau)}{\partial x_1}\right|_{x=0} = \kappa_d(K_m c_d(\tau) - c_m(0,\tau)) \tag{25}$$

$$\frac{dc_d(\tau)}{d\tau} = \frac{1}{V_{dN}K_m}\left.\frac{\partial c_m(x_1,t)}{\partial x_1}\right|_{x_1=0} \tag{26}$$

$$-\left.\frac{\partial c_m(x_1,\tau)}{\partial x_1}\right|_{x_1=1} = \kappa_{ve}\left(c_m(h_m,\tau) - \frac{K_m c_r(\tau)}{K_r}\right) \tag{27}$$

$$\frac{dc_r(\tau)}{d\tau} = -\frac{V_m}{V_r}\left.\frac{\partial c_m(x_1,\tau)}{\partial x_1}\right|_{x=1} - \frac{Cl_{rN}}{V_{rN}} c_r(\tau) \tag{28}$$

$$c_d(0) = \frac{1}{K_m} \tag{29}$$

$$c_r(0) = 0 \tag{30}$$

using the following definitions:

$$V_{dN} = \frac{V_d}{V_m K_m}; t_d = \frac{h_m^2}{D_m}; k_p^{sc} = \frac{K_m D_m}{h_m}; \kappa_{ve} = \frac{k_p^{ve}}{k_p^{sc}}; Cl_{rN} = \frac{Cl_r K_r}{k_p^{sc} A};$$
$$V_{rN} = \frac{V_r K_r}{V_m K_m}; V_m = Ah_m; V_d = Ah_d; x_1 = \frac{x}{h_m}; \tau = \frac{t}{t_d}; c_m = \frac{C_m}{K_m C_{d0}};$$
$$c_d = \frac{C_d}{K_m C_{d0}}; \kappa_d = \frac{k_p^d}{k_p^{sc}}; V_{\frac{m}{r}} = \frac{V_m}{V_r} = \frac{K_r}{K_m V_{rN}}$$

The flux is given by

$$j(\tau) = -\frac{K_m D_m C_{d0}}{h_m}\left.\frac{\partial c_m(x_1,\tau)}{\partial x_1}\right|_{x_1=1} = -k_p^{sc} C_{d0}\left.\frac{\partial c_m(x_1,\tau)}{\partial x_1}\right|_{x_1=1} \tag{31}$$

A dimensionless delivery rate is used:

$$\frac{j(\tau)}{k_p^{sc} C_{d0}} = -\left.\frac{\partial c_m(x_1,\tau)}{\partial x_1}\right|_{x_1=1} \tag{32}$$

3.1.2. Derivation of t_{jmax} and j_{max} for Model 1

After applying the Laplace operator to Eqs. (23) through (30) and (32), the following equation was obtained:

$$\frac{J(s_d)}{k_p^{sc}C_{d0}} = \frac{P(s_d)}{Q(s_d)} \tag{33}$$

where

$$P(s_d) = 2e^{\sqrt{s_d}}\kappa_d V_{dN} K_r \kappa_{ve}(Cl_{rN} + s_d V_{rN}) \tag{34}$$

and

$$Q(s_d) = \begin{cases} (-\sqrt{s_d}\kappa_d V_{dN} K_m + \kappa_d + s_d V_{dN} K_m)\left(Cl_{rN} K_r(\kappa_{ve} - \sqrt{s_d}) - \sqrt{s_d} V_{rN}\left(K_m \kappa_{ve} V_{\frac{m}{r}} + K_r(s_d - \sqrt{s_d}\kappa_{ve})\right)\right) + \\ e^{2\sqrt{s_d}}(\sqrt{s_d}\kappa_d V_{dN} K_m + \kappa_d + s_d V_{dN} K_m)\left(Cl_{rN} K_r(\sqrt{s_d} + \kappa_{ve}) + \sqrt{s_d} V_{rN}\left(K_m \kappa_{ve} V_{\frac{m}{r}} + K_r(\sqrt{s_d}\kappa_{ve} + s_d)\right)\right) \end{cases} \tag{35}$$

In this context, s_d represents a dimensionless Laplace variable defined by $s_d = s\frac{h_m^2}{D_m}$ where s is the dimensional Laplace variable with unit of 1/time. The maximum flux is (Eq. (7))

$$\frac{j_{max}}{k_p^{sc}C_{d0}} = \frac{\left(\frac{a}{b}\right)^{-\frac{b}{a-b}}k}{a} \tag{36}$$

and the peak time is

$$\tau_{j\,max} = \frac{\ln(a/b)}{a-b} \tag{37}$$

where a and b are calculated from Eqs. (11) and (12) (see Appendix A for a detailed derivation).

3.1.3. Calculation of τ_{jmax} and $\frac{j_{max}}{k_p^{sc}C_{d0}}$ for specific parameter values

Consider the parameter values $K_r = 0.5$, $K_m = 1$, $\kappa_d = 1$, $V_{dN} = 1$, $\kappa_{ve} = 0.1$, $V_{rN} = 1$ and $Cl_{rN} = 2$. The following expressions and constants were obtained:

$$\frac{J(s_d)}{k_p^{sc}C_{d0}} = \frac{0.2e^{\sqrt{s_d}}(s_d + 2.)}{\left[\begin{array}{l} -1.{s_d}^{5/2} - 3.2{s_d}^{3/2} + 1.1{s_d}^2 + e^{2\sqrt{s_d}}\left(1.{s_d}^{5/2} + 3.2{s_d}^{3/2} + 1.1{s_d}^2 + 2.4s_d + 2.3\sqrt{s_d} + 0.2\right) + \\ 2.4s_d - 2.3\sqrt{s_d} + 0.2 \end{array}\right]} \tag{38}$$

$$\frac{J(s_d)}{k_p^{sc}C_{d0}} \approx \frac{1.0}{1.0 + 23.5s_d + 17.7{s_d}^2} \tag{39}$$

$a = 1.28$, $b = 0.044$, $k = 0.056$, $\tau_{jmax} = 2.72$ and $\frac{j_{max}}{k_p^{sc}C_{d0}} = 0.039$. To compare the two profiles (Fig. 2), the inverse Laplace transform of Eq. (38) was computed using a numerical method.(Abate and Valkó, 2004).

3.2. Drug absorption from a transdermal patch (Simon, 2007)

3.2.1. Governing equations for the patch-skin model (Model 2)

The system is represented by a patch, a skin membrane and the capillary. The drug concentrations in the patch and the skin are represented by C_1 and C_2, respectively (Fig. 1). In a previous contribution, the following PDEs were used (Simon and Loney, 2005):

$$\frac{\partial C_1}{\partial t} = D_1\frac{\partial^2 C_1}{\partial x^2}; -h_1 < x < 0 \tag{40}$$

and

$$\frac{\partial C_2}{\partial t} = D_2\frac{\partial^2 C_2}{\partial x^2}; 0 < x < h_2 \tag{41}$$

The initial conditions are

$$C_1(x,0) = C_{10}; -h_1 < x < 0 \tag{42}$$

and

$$C_2(x,0) = 0; 0 < x < h_2 \tag{43}$$

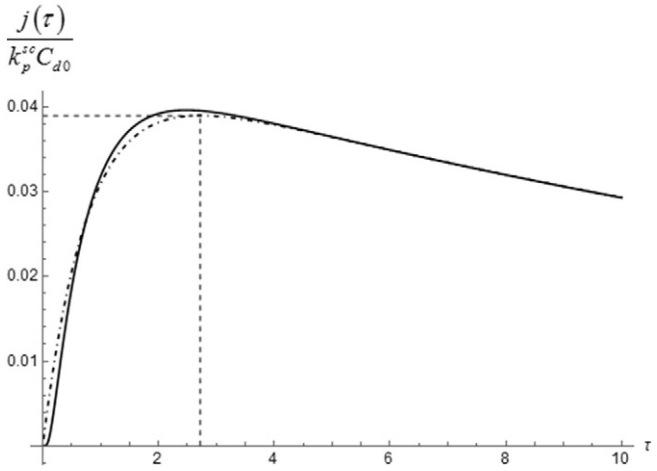

Fig. 2. Actual (—) and estimated (— ● — ● —) normalized flux for Model 1. The peak time and maximum flux are represented by the rectangle.

The boundary conditions are

$$\frac{\partial C_1(-h_1,t)}{\partial x} = 0 \tag{44}$$

$$\frac{D_1 \partial C_1(0,t)}{\partial x} = \frac{D_2 \partial C_2(0,t)}{\partial x} \tag{45}$$

$$K_m C_1(0,t) = C_2(0,t) \tag{46}$$

$$-\frac{D_2 \partial C_2(h_2,t)}{\partial x} = K_{cl} C_2(h_2,t) \tag{47}$$

where K_m stands for the patch-skin partition coefficient; D_1 and D_2 are the drug diffusion coefficients in the patch and the skin, respectively; K_{cl} is the skin-capillary clearance per unit area of drug; h_1 is the thickness of the vehicle; h_2 is the skin thickness; C_{20} is the initial drug concentration in the skin. Eqs. (40)–(43) are the transport equations with the initial concentration values. Eqs. (44)–(47) describe the zero-flux condition at $x = -h_1$, the flux continuity relation at the patch-skin interface, the equilibrium partition and solute elimination from the skin into the system circulation, respectively. The delivery rate is

$$j(t) = -\frac{D_2 \partial C_2(h_2,t)}{\partial x} \tag{48}$$

3.2.2. Derivation of t_{jmax} and j_{max} for Model 2

The system formed by Eqs. (40)–(47) is solved in the Laplace domain to yield the following delivery rate:

$$J(s) = \frac{c_{10}\sqrt{D_1 D_2} K_{\mathrm{cl}} K_m \sinh\left(h_1\sqrt{\frac{s}{D_1}}\right)}{\sqrt{s}\left(\begin{array}{l}\cosh\left(h_1\sqrt{\frac{s}{D_1}}\right)\left(\sqrt{D_2} K_{\mathrm{cl}} K_m \cosh\left(h_2\sqrt{\frac{s}{D_2}}\right) + D_2\sqrt{s} K_m \sinh\left(h_2\sqrt{\frac{s}{D_2}}\right)\right)+ \\ \sinh\left(h_1\sqrt{\frac{s}{D_1}}\right)\left(\sqrt{D_1} K_{\mathrm{cl}} \sinh\left(h_2\sqrt{\frac{s}{D_2}}\right) + \sqrt{D_1 D_2 s}\cosh\left(h_2\sqrt{\frac{s}{D_2}}\right)\right)\end{array}\right)} \tag{49}$$

The maximum flux is (Eq. (7))

$$j_{\max} = \frac{\left(\frac{a}{b}\right)^{-\frac{b}{a-b}} k}{a} \tag{50}$$

and the peak time is

$$t_{j\max} = \frac{\ln(a/b)}{a-b} \tag{51}$$

where a and b are obtained by Eqs. (11) and (12) (see Appendix B for a detailed derivation).

3.2.3. Calculation of t_{jmax} and j_{max} for given parameter values

The parameter values $h_1 = 0.004$ cm, $h_2 = 0.0125$ cm, $K_{cl} = 12.5$ cm/h, $c_{10} = 200{,}000$ μg/cm^3, $D_1 = 9.72\times10^{-6}$ cm^2/h, $D_2 = 2.812\times10^{-6}$ cm^2/h and $K_m = 1$ were employed for the simulation. The following expressions and parameter values were calculated:

$$J(s) = \frac{13.07\sinh\left[1.28\sqrt{s}\right]}{\sqrt{s}\left(\begin{array}{l}\sinh\left[1.28\sqrt{s}\right]\left(5.23\times10^{-6}\sqrt{s}\cosh\left[7.45\sqrt{s}\right]+0.039\sinh\left[7.45\sqrt{s}\right]\right)+\\ \cosh\left[1.28\sqrt{s}\right]\left(0.021\cosh\left[7.45\sqrt{s}\right]+2.81\times10^{-6}\sqrt{s}\sinh\left[7.45\sqrt{s}\right]\right)\end{array}\right)} \tag{52}$$

$$J(s)\approx\frac{2.59}{(s+0.12)(s+0.026)} \tag{53}$$

$a = 0.12$, $b = 0.026$, $k = 2.59$, $t_{jmax} = 15.93$ h and $j_{max} = 13.84$ μg/cm^2 h. The two flux profiles are plotted in Fig. 3.

3.3. A dissolution model involving first-order dissolution (McGinty et al., 2015)

3.3.1. Governing equations for the diffusion-dissolution model (Model 3)

A situation is described where a drug is dissolved with a finite dissolution rate in a volume of fluid. The governing equations are (Fig. 1)

$$\frac{\partial C_f(x,t)}{\partial t} = D_p\frac{\partial^2 C_f(x,t)}{\partial x^2} + K_1 C_b(t),\quad 0<x<L_p,\ t>0 \tag{54}$$

$$\frac{dC_b(t)}{dt} = -K_1 C_b(t),\quad 0<x<L_p,\ t>0 \tag{55}$$

$$C_b(0) = C_{b0},\quad 0\le x\le L_p \tag{56}$$

$$C_f(x,0) = 0,\quad 0\le x\le L_p \tag{57}$$

$$-D_p\frac{\partial C_f(0,t)}{\partial x} = 0,\quad t>0 \tag{58}$$

$$C_f(L_p,t) = 0,\quad t>0 \tag{59}$$

Eq. (54) is a transport equation which involves dissolution of a crystalline drug and diffusion through a medium of length L_p. Dissolution of the drug is realized through a first-order process with a rate constant K_1 (Eq. (55)). The free drug concentration is denoted by C_f; D_p is the diffusion coefficient. The initial conditions are stated in Eqs. (56) and (57). No drug leaves the region at $x = 0$ (Eq. (58)). An infinite sink boundary condition is imposed at $x = L_p$. The flux is

$$j(t) = -D_p\frac{\partial C_f(L_p,t)}{\partial x},\quad t>0 \tag{60}$$

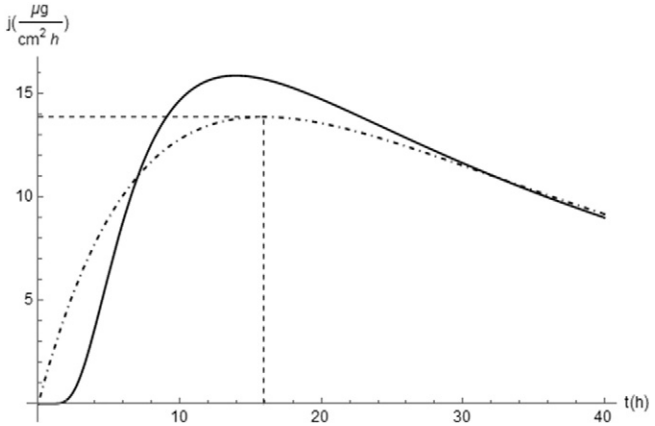

Fig. 3. Actual (—) and estimated (— ● — ● —) delivery rate for Model 2. The peak time and maximum flux are shown by the rectangle.

3.3.2. Derivation of t_{jmax} and j_{max} for Model 3

It can be shown that the Laplace transformed flux is

$$J(s) = \frac{K_1 c_{b0} D_p \tanh\left(L_p\sqrt{\frac{s}{D_p}}\right)}{(K_1 + s)\sqrt{sD_p}} \tag{61}$$

The maximum flux and peak time are Eqs. (50) and (51) where a and b are derived following the procedure outlined in Appendix C.

3.3.3. Calculation of t_{jmax} and j_{max} for specific parameter values

The following parameter values were used for the simulation: $D_p = 3.6\times10^{-9}$ cm^2/h, $L_p = 10^{-3}$ cm, $K_1 = 0.036$ h^{-1} and $c_{b0} = 1.0$ μg/cm^3.

$$J(s) = \frac{2.16\times10^{-6}\tanh(16.67\sqrt{s})}{\sqrt{s}(s+0.036)} \tag{62}$$

$$J(s) \approx \frac{1.16\times10^{-6}}{(s+0.13)(s+0.0089)} \tag{63}$$

$a = 0.13$, $b = 0.0089$, $k = 1.16\times10^{-6}$, $t_{jmax} = 21.98$ h and $j_{max} = 7.30\times10^{-6}$ μg/cm^2 h. The two flux profiles are displayed in Fig. 4.

The examples listed above show the applications of a method to estimate the peak time and maximum flux from laboratory data. These theoretical models were first developed for controlled-release systems by applying the principle of mass conservation. They represent mechanisms that govern the drug-release mechanisms, including partitioning and diffusion through the membrane. As abstractions of complex phenomena, the mathematical equations involve certain assumptions, such as an equilibrium partitioning condition at the interface between two adjacent regions and a constant diffusion coefficient. The model is accepted if it represents the experimental observations to a desired degree of accuracy. At this point, the construct becomes part of a decision support system that researchers can exploit to predict, for instance, in-vivo drug profiles, when only in-vivo information is available (Emami, 2006). Such efforts have been used to design experiments and extract meaningful performance metrics for the data (e.g., the lag time and effective time constant). In a similar fashion, the procedure, outlined above, provides clinicians with a tool to interpret observed dynamics and to relate t_{jmax} and j_{max} to relevant process parameters, such as the diffusion coefficient. Its accuracy depends on how well the second-order model represents the original PDE system. The transdermal patch exhibits a relatively long lag time, which is not captured by the empirical model. As a result, determination of j_{max} is less accurate when compared to Models 1 and 3. Even in this case, it is worth noting that the procedure outlined would be different if the main objective was to offer a solution that simulates the process dynamics accurately. Such a goal could be met by applying an orthogonal collocation or a centered finite-difference based approach. The focus is to develop a a-priori prediction technique which would help investigators design a transdermal patch with desirable properties (e.g., diffusion coefficient and thickness), or features that satisfy Eqs. (50) and (51). The theoretical tool could be applied for the selection and optimization of lead formulation candidates. This effort would reduce the number of laboratory experiments, thereby saving drug manufacturers' time and effort.

As in the case of compartmental pharmacokinetic analyses, one needs to weigh the benefits of the new computational tool against a lower-order, but practical, description of the phenomenon. In biomedecine, linear compartmental analyses are useful for investigating drug kinetics in humans and for designing dosage regimens (Cherruault, 1986). The calculated regimens are based on optimal control techniques, which are well-established for linear systems. A rigorous description of drug transport through the body would make it difficult to solve the optimal control problem. A similar approach is taken in process control where empirical models are deemed adequate for the design of effective control systems (Seborg, 2011; Simon, 2013). The approach is applicable to linear drug delivery models showing a maximum flux or a maximum plasma drug concentration. Examples of such systems are the in-vitro release of timolol from polymer matrices (Kubota et al., 2002) and the permeation of testosterone through the epidermis (Anissimov and Roberts, 2001).

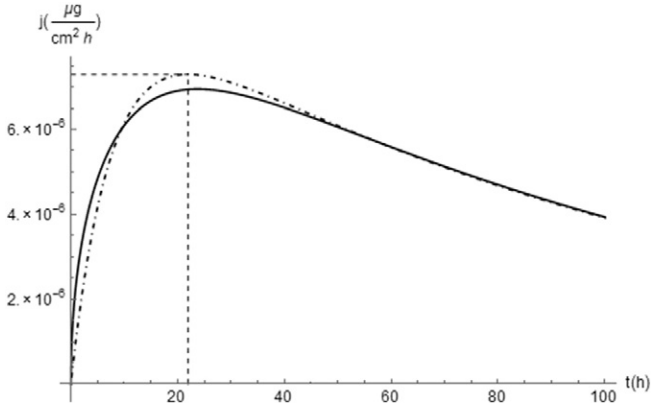

Fig. 4. Actual (—) and estimated (— ● — ● —) delivery rate for Model 3. The peak time and maximum flux are shown by the rectangle.

4. Conclusions

A method was designed to compute the peak flux and time-to-peak for topically-applied drugs. The delivery rate through the skin was zero at the beginning of the administration, reached a maximum value and then vanished at a very long time. To help with the analysis, the Laplace-transformed flux was first approximated by an empirical process. The roots of the reciprocal of the transformed function were obtained by producing a second-order power series expansion. The resulting expressions allowed calculations of the performance indicators. Three cases were presented to illustrate the technique. The first example included transport from a donor into a receiver compartment. The mechanism involved the transfer of the drug molecules from the donor cell to the surface of the skin, followed by permeation through the skin layers and release into the receiver chamber. The second system, comprised of a patch, the skin and capillary, was modeled by two partial differential equations. The final test consisted of a crystalline drug dissolving in a finite volume of liquid before diffusing through a medium. In all three cases, closed-formed expressions were derived that relate the peak flux and time-to-peak to critical process parameters, such as the diffusion and partition coefficients. The method becomes less accurate for systems with a longer lag time.

Appendix A. Detailed derivation of $t_{j\max}$ and $j_{\max}$ for Model 1

The software, Mathematica® (Wolfram Research, Inc., Champaign, Illinois), was used to perform the symbolic computation. Application of Eq. (10) leads to

$$\frac{k_p^{sc} C_{d0}}{J(s_d)} \approx c_0 + c_1 s_d + c_2 {s_d}^2 \tag{A.1}$$

with

$$c_0 = \frac{1}{V_{\mathrm{dN}}} \tag{A.2}$$

$$c_1 = \left(\frac{K_m V_{\mathrm{rN}} V_{\frac{m}{r}}}{\mathrm{Cl}_{\mathrm{rN}} V_{\mathrm{dN}} K_r} + \frac{K_m^2 V_{\mathrm{rN}} V_{\frac{m}{r}}}{\mathrm{Cl}_{\mathrm{rN}} K_r} + \frac{K_m}{\kappa_d} + \frac{1}{V_{\mathrm{dN}} \kappa_{\mathrm{ve}}} + \frac{1}{2V_{\mathrm{dN}}} + \frac{K_m}{\kappa_{\mathrm{ve}}} + K_m \right) \tag{A.3}$$

and

$$c_2 = \frac{\left(\begin{array}{l} 12\mathrm{Cl}_{\mathrm{rN}}^2 \kappa_d V_{\mathrm{dN}} K_m K_r + 4\mathrm{Cl}_{\mathrm{rN}}^2 \kappa_d V_{\mathrm{dN}} K_m K_r \kappa_{\mathrm{ve}} + 12\mathrm{Cl}_{\mathrm{rN}} \kappa_d V_{\mathrm{dN}} K_m^2 V_{\mathrm{rN}} \kappa_{\mathrm{ve}} V_{\frac{m}{r}} + \\ 4\mathrm{Cl}_{\mathrm{rN}} \kappa_d K_m V_{\mathrm{rN}} \kappa_{\mathrm{ve}} V_{\frac{m}{r}} + 4\mathrm{Cl}_{\mathrm{rN}}^2 \kappa_d K_r + \mathrm{Cl}_{\mathrm{rN}}^2 \kappa_d K_r \kappa_{\mathrm{ve}} + 12\mathrm{Cl}_{\mathrm{rN}}^2 V_{\mathrm{dN}} K_m K_r \kappa_{\mathrm{ve}} + \\ 24\mathrm{Cl}_{\mathrm{rN}} V_{\mathrm{dN}} K_m^2 V_{\mathrm{rN}} \kappa_{\mathrm{ve}} V_{\frac{m}{r}} + 24\mathrm{Cl}_{\mathrm{rN}}^2 V_{\mathrm{dN}} K_m K_r - 24\kappa_d V_{\mathrm{dN}} K_m^2 V_{\mathrm{rN}}^2 \kappa_{\mathrm{ve}} V_{\frac{m}{r}} - 24\kappa_d K_m V_{\mathrm{rN}}^2 \kappa_{\mathrm{ve}} V_{\frac{m}{r}} \end{array} \right)}{24\mathrm{Cl}_{\mathrm{rN}}^2 \kappa_d V_{\mathrm{dN}} K_r \kappa_{\mathrm{ve}}} \tag{A.4}$$

After taking the limit of $\frac{J(s_d)}{k_p^{sc} C_{d0}}$ as s approaches infinity, we obtain

$$\lim_{s_d \to 0} \left(\frac{J(s_d)}{k_p^{sc} C_{d0}} \right) = \lim_{s \to 0} \left(\frac{P(s_d)}{Q(s_d)} \right) = V_{dN} \tag{A.5}$$

Therefore, by using Eq. (9), we have

$$k = abV_{dN} \tag{A.6}$$

The maximum flux is (Eq. (7))

$$\frac{j_{\max}}{k_p^{sc} C_{d0}} = \frac{\left(\frac{a}{b}\right)^{-\frac{b}{a-b}} k}{a} \tag{A.7}$$

and the peak time is

$$\tau_{j\max} = \frac{\ln(a/b)}{a-b} \tag{A.8}$$

where a and b are calculated from Eqs. (11) and (12). The maximum flux is (Eq. (7))

$$\frac{j_{\max}}{k_p^{sc} C_{d0}} = \frac{\left(\frac{a}{b}\right)^{-\frac{b}{a-b}} k}{a} \tag{A.9}$$

and the peak time is given by

$$\tau_{j\max} = \frac{\ln(a/b)}{a-b} \tag{A.10}$$

where a and b are computed from Eqs. (11) and (12).

Appendix B. Detailed derivation of t_{jmax} and j_{max} for Model 2

Application of Eq. (10) leads to

$$\frac{1}{J(s)} \approx c_0 + c_1 s + c_2 s^2 \tag{B.1}$$

with

$$c_0 = \frac{1}{h_1 c_{10}} \tag{B.2}$$

$$c_1 = \frac{2D_2 h_1^2 K_{cl} K_m + 3D_1 h_2 K_m (h_2 K_{cl} + 2D_2) + 6D_1 h_1 (h_2 K_{cl} + D_2)}{6 c_{10} D_1 D_2 h_1 K_{cl} K_m} \tag{B.3}$$

and

$$c_2 = \frac{\left[\begin{array}{l} -8D_2^2 h_1^4 K_{cl} K_m + 60 D_1 D_2 h_2 h_1^2 K_m (h_2 K_{cl} + 2D_2) + \\ 15 D_1^2 h_2^3 K_m (h_2 K_{cl} + 4D_2) + 60 D_1^2 h_2^2 h_1 (h_2 K_{cl} + 3D_2) \end{array}\right]}{360 c_{10} D_1^2 D_2^2 h_1 K_{cl} K_m} \tag{B.4}$$

after running the Mathematica® code Chop[Normal[Series[1/J[s],{s,0,2}]]]. As a result,

$$\lim_{s \to 0} J(s) = h_1 c_{10} \tag{B.5}$$

After applying Eq. (9), we have

$$k = abh_1 c_{10} \tag{B.6}$$

The maximum flux is (Eq. (7))

$$j_{max} = \frac{\left(\frac{a}{b}\right)^{-\frac{b}{a-b}} k}{a} \tag{B.7}$$

and the peak time is

$$t_{jmax} = \frac{\ln(a/b)}{a-b} \tag{B.8}$$

where a and b are obtained by Eqs. (11) and (12).

Appendix C. Detailed derivation of t_{jmax} and j_{max} for Model 3

Eq. (10) is applied to get

$$\frac{1}{J(s)} \approx c_0 + c_1 s + c_2 s^2 \tag{C.1}$$

with

$$c_0 = \frac{1}{c_{b0} L_p} \tag{C.2}$$

$$c_1 = \frac{\frac{L_p}{3D_p} + \frac{1}{K_1 L_p}}{c_{b0}} \tag{C.3}$$

and

$$c_2 = \frac{15 D_p L_p - K_1 L_p^3}{45 K_1 c_{b0} D_p^2} \tag{C.4}$$

Therefore,

$$\lim_{s \to 0} J(s) = c_{b0} L_p \tag{C.5}$$

After applying Eq. (9), we have

$$k = abc_{b0} L_p \tag{C.6}$$

The maximum flux is defined by Eq. (7)

$$j_{max} = \frac{\left(\frac{a}{b}\right)^{-\frac{b}{a-b}} k}{a} \tag{C.7}$$

and the peak time is

$$t_{jmax} = \frac{\ln(a/b)}{a-b} \tag{C.8}$$

where a and b are defined by Eqs. (11) and (12).

References

Abate, J., Valkó, P.P., 2004. Multi-precision Laplace transform inversion. Int. J. Numer. Methods Eng. 60, 979–993.

Allen, L.V., Ansel, H.C., 2014. Ansel's Pharmaceutical Dosage Forms and Drug Delivery Systems. Tenth edition. ed. Wolters Kluwer Health, Philadelphia.

Anissimov, Y.G., Roberts, M.S., 2001. Diffusion modeling of percutaneous absorption kinetics: 2. Finite vehicle volume and solvent deposited solids. J. Pharm. Sci. 90, 504–520.

Cherruault, Y., 1986. Mathematical Modelling in Biomedicine: Optimal Control of Biomedical Systems. D. Reidel Pub. Co., Dordrecht, Holland.

Collins, R., 1980. The choice of an effective time constant for diffusive processes in finite systems (thermal conduction and sputtering examples). J. Phys. D. Appl. Phys. 13, 1935.

Crank, J., 1975. The Mathematics of Diffusion. second ed. Clarendon Press, Oxford, Eng.

Edward, A., Prausnitz, M.R., 2001. Predicted permeability of the cornea to topical drugs. Pharm. Res. 18, 1497–1508.

Emami, J., 2006. In vitro - in vivo correlation: from theory to applications. J. Pharm. Pharm. Sci. 9, 169–189.

Gutman, J., Green, M., Durand, S., Rojas, O.V., Ganguly, B., Quezada, W.M., Utz, G.C., Slutsker, L., Ruebush III, T.K., Bacon, D.J., 2009. Mefloquine pharmacokinetics and mefloquine-artesunate effectiveness in Peruvian patients with uncomplicated *Plasmodium falciparum* malaria. Malar. J. 8, 58.

Hedaya, M.A., 2012. Basic Pharmacokinetics. second ed. Taylor & Francis/CRC Press, Boca Raton.

Kubota, K., Dey, F., Matar, S.A., Twizell, E.H., 2002. A repeated-dose model of percutaneous drug absorption. Appl. Math. Model. 26, 529–544.

McCarley, K.D., Bunge, A.L., 2001. Pharmacokinetic models of dermal absorption. J. Pharm. Sci. 90, 1699–1719.

McGinty, S., McKee, S., McCormick, C., Wheel, M., 2015. Release mechanism and parameter estimation in drug-eluting stent systems: analytical solutions of drug release and tissue transport. Math Med. Biol. 32, 163–186.

Scheuplein, R.J., Ross, L.W., 1974. Mechanism of percutaneous absorption. V. Percutaneous absorption of solvent deposited solids. J. Invest. Dermatol. 62, 353–360.

Seborg, D.E., 2011. Process Dynamics and Control. third ed. John Wiley & Sons, Inc., Hoboken, N.J.

Simon, L., 2007. Repeated applications of a transdermal patch: analytical solution and optimal control of the delivery rate. Math. Biosci. 209, 593–607.

Simon, L., 2009. Timely drug delivery from controlled-release devices: dynamic analysis and novel design concepts. Math. Biosci. 217, 151–158.

Simon, L., 2013. Control of Biological and Drug-delivery Systems for Chemical, Biomedical, and Pharmaceutical Engineering. Wiley, Hoboken, N.J.

Simon, L., Loney, N.W., 2005. An analytical solution for percutaneous drug absorption: application and removal of the vehicle. Math. Biosci. 197, 119–139.

Urso, R., Blardi, P., Giorgi, G., 2002. A short introduction to pharmacokinetics. Eur. Rev. Med. Pharmacol. Sci. 6, 33–44.

Walters, K.A., 2002. Dermatological and Transdermal Formulations. M. Dekker, New York.

Weidekamm, E., Rusing, G., Caplain, H., Sorgel, F., Crevoisier, C., 1998. Lack of bioequivalence of a generic mefloquine tablet with the standard product. Eur. J. Clin. Pharmacol. 54, 615–619.